

Supporting Information

Islam et al. 10.1073/pnas.0802699105

	1	10	20	30	40	50	58	
Wild-type:	RPDFCLEPP	YTGPK	ARIIRYFYN	AKAGLCQ	TFVYGGCR	AKRNNFKS	AEDCMRTC	CGGA
BPTI-[5,55]:	RPDFCLEPP	YTGPAK	ARIIRYFYN	AKAGLAQ	TFVYGGAR	AKRNNFKS	AEDALRTC	CGGA
BPTI-[5,55]st:	RPDFCLEPP	YTGPK	ARIIRYFYN	AKAGLAQ	TFVYGGAR	AKRNNFKS	AEDALRTC	CGGA
BPTI-21:	RP	AFCLEPP	YAGPK	ARIIRYFYN	AAAGAAQ	AFVYGGAR	AKRNNFAS	AADALAACAAA
BPTI-20st:	RP	AFCLEPP	YAGPK	ARIIRYFYN	AAAGAAQ	AFVYGGAR	AKRNNFAS	AADALAACAAA
	<u>3₁₀-Helix</u>			<u>β-Strand 1</u>		<u>β-Strand 2</u>		<u>α-Helix</u>

Fig. S1. Sequences of the wild-type BPTI, BPTI-[5,55], BPTI-[5,55]st, BPTI-21, and BPTI-20st. Alanines are shown in red. A14G was introduced to stabilize the BPTI-21 and BPTI-[5,55], and M52L for avoiding cleavage by cyanogen bromide during the purification protocol. BPTI-[5,55] is a single-disulfide-bonded variant with the remaining two S-S bonds substituted to alanines. Simplified BPTI-21 sequence contains a total of 14 alanine substitutions, of which 3 are buried and 2 are partially buried.

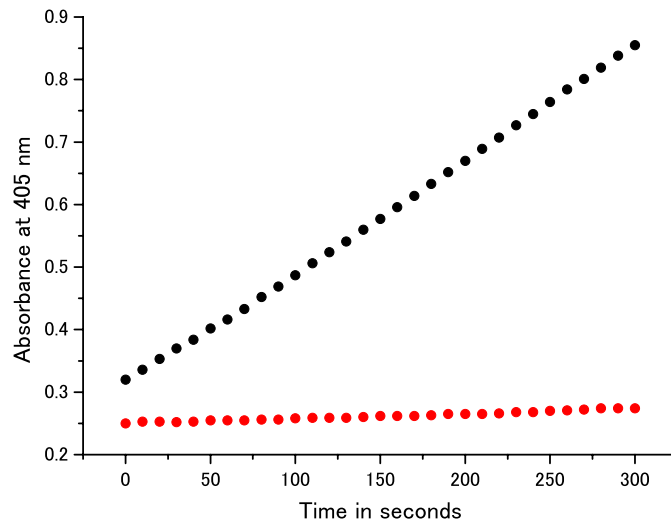


Fig. S2. Trypsin inhibition activity of BPTI variants. The trypsin inhibition activity of the BPTI variants was assayed by monitoring the hydrolysis of *N*^α-benzoyl-DL-arginine *p*-nitroanilide (BAPA) in 0.2 M phosphate buffer (pH 7.0) at room temperature [Kassell, B (1970) *Method Enzymol* 19:844–852]. Black filled circles represent the activity of trypsin on *N*^α-benzoyl-DL-arginine *p*-nitroanilide (BAPA) in absence of BPTI and filled red circles represent the activity of trypsin BAPA in presence of BPTI-20st at equimolar concentration (280 nM) measured at 405 nm over 5 min.

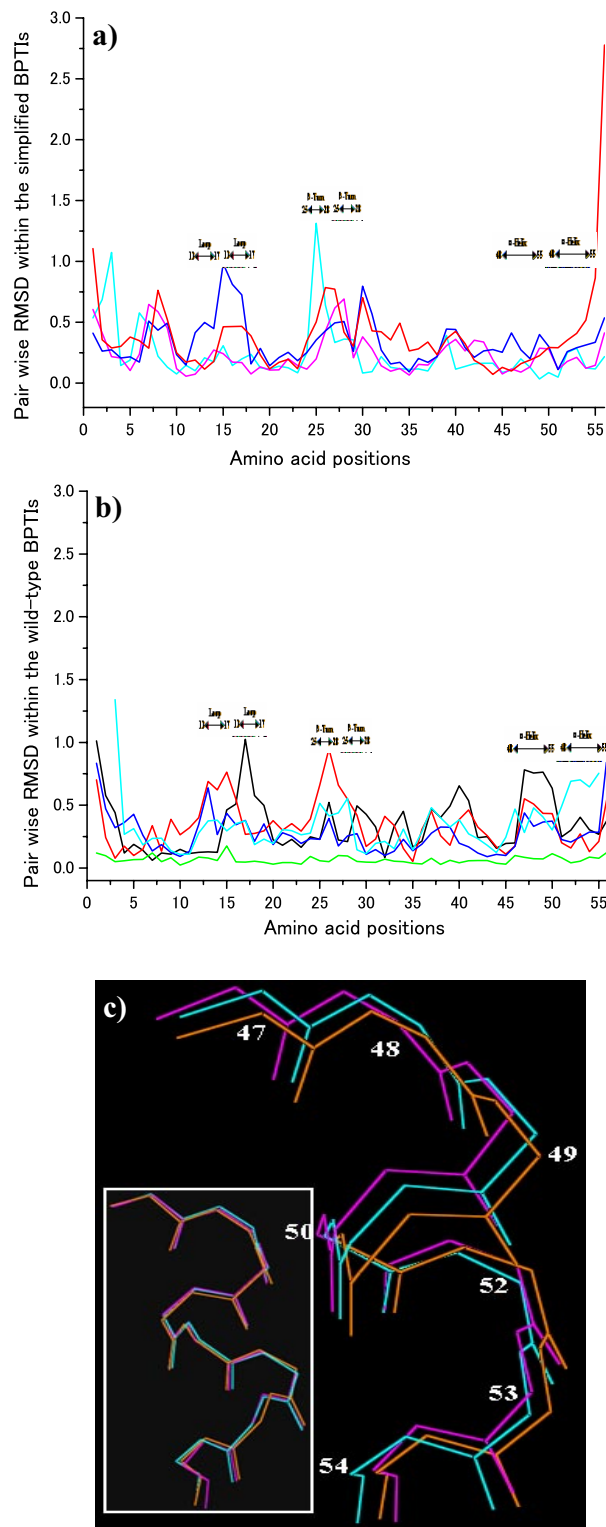


Fig. 53. Structural variations within the wild-type and simplified BPTIs. (a) Pairwise RMSD among the chains in the asymmetric units. Cyan line for chain 1/chain 2 of BPTI-[5,55]st, violet, blue, and red lines for chain 1/chain 2, chain 1/chain 3, and chain 1/chain 4, respectively of BPTI-20st. (b) Pairwise RMSD among the wild-type structures. Here, 5PTI is used as the reference wild-type structure. Black, red, green, blue, and cyan lines represent 4PTI, 6PTI, 9PTI, 1G6X, and 2FI3, respectively. (c) Superimposed structures of the 47~54 α -helix region. The backbone structures of the 47~54 α -helix region observed upon global superimposition of BPTI-20st and BPTI[5,55]st onto 5PTI (RMSD 0.45~1.29 Å). Local superimposed structures of the 47~54 α -helix region (RMSD 0.17 Å) are shown in *Inset*.

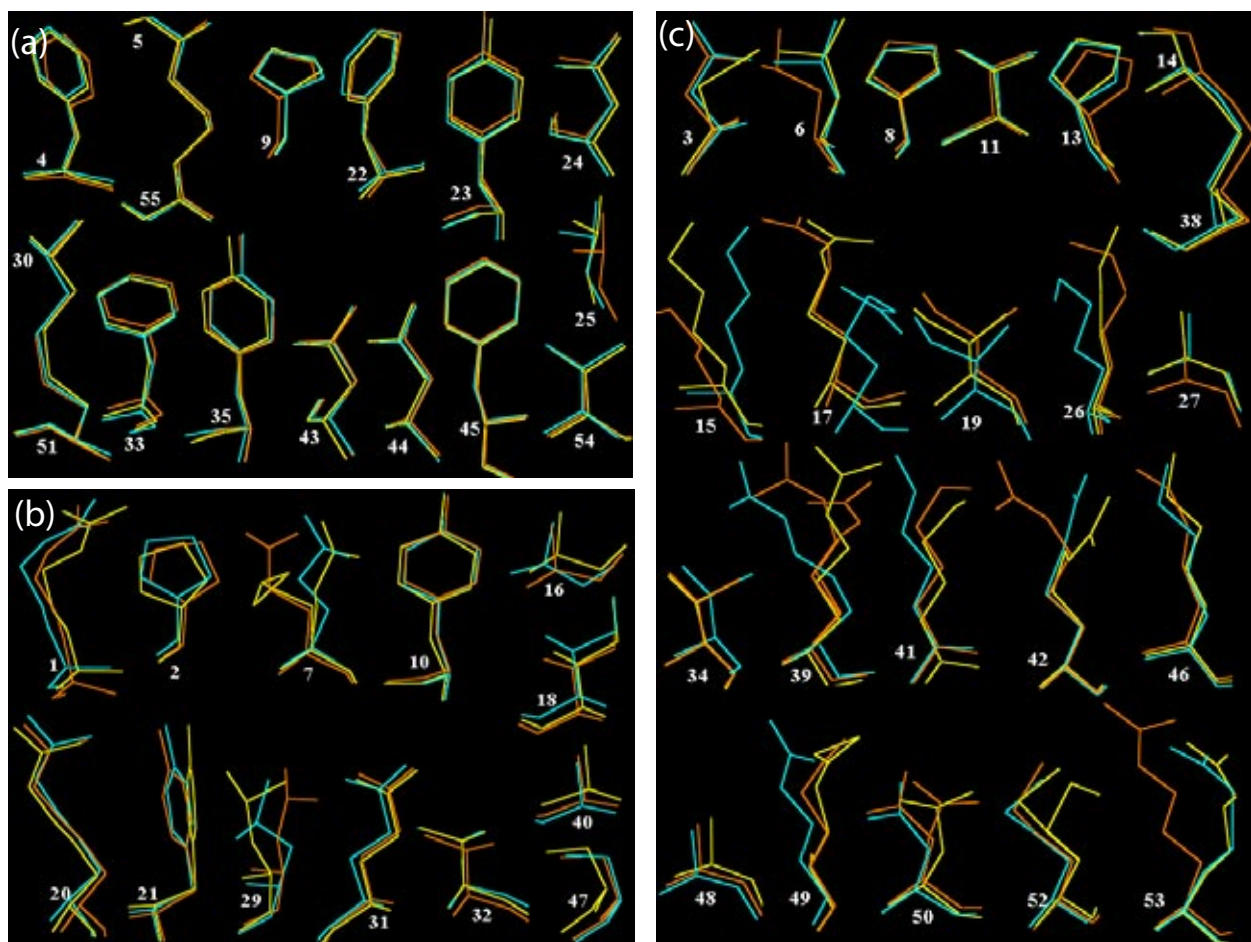


Fig. S4. Side-chain conformations in wild-type BPTI structures. Side-chain structures of residues buried (ASA 0~30%) (a), partially buried (ASA 30~50%) (b) and surface-exposed (ASA 50~70%) (c). Yellow, cyan, and orange, respectively, for 5PTI, 4PTI, and 6PTI. Figures were generated by using PyMOL graphics (www.pymol.org).

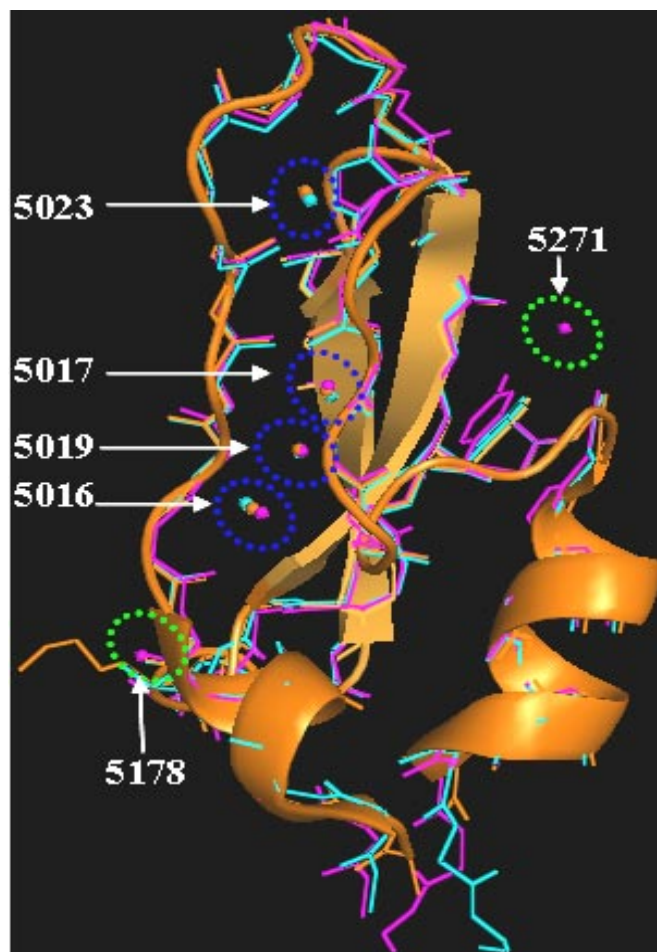


Fig. S5. Conserved structural water molecules. Four completely buried water molecules conserved in several wild-type BPTI structures (marked by blue circles) are also conserved in simplified BPTI structures. In addition, two new waters are observed only in BPTI-20st structures (green circle); one is close to the 25~28 β -turn region and the other is hydrogen-bonded to the side-chain atom of Tyr-21, which is assigned in a slightly shifted configuration in BPTI-20st. Identities of water molecules are taken from BPTI-20st. Orange, cyan, and pink represent, respectively, wild type, BPTI-[5,55]st, and BPTI-20st. The figure was generated with PyMOL (www.pymol.org).

Table S1. Structural variations among wild-type, reference, and simplified BPTIs

RMSD, Å	Structure pair					
	4PTI/5PTI	4PTI/6PTI	4PTI/9PTI	5PTI/-20 st	5PTI/-[5,55]st	-20st/-[5,55]st
C ^α	0.398	0.417	0.403	0.565	0.469	0.552
BB	0.402	0.436	0.417	0.551	0.480	0.534
All	1.104	1.155	1.068	0.810	0.967	1.05

4PTI (1), 5PTI (2), 6PTI (3), and 9PTI (4) are the PDB ID codes of wild-type BPTI structures.

1. Bolognesi M, *et al.* (1982) Three-dimensional structure of the complex between pancreatic secretory trypsin inhibitor (Kazal type) and trypsinogen at 1.8 Å resolution. Structure solution, crystallographic refinement and preliminary structural interpretation. *J Mol Biol* 162:839–868.
2. Wlodawer A, Nachman J, Gilliland GL, Gallagher W, Woodward C (1987) Structure of form III crystals of bovine pancreatic trypsin inhibitor. *J Mol Biol* 198:469–480.
3. Wlodawer A, Walter J, Huber R, Sjolín L (1984) Structure of bovine pancreatic trypsin inhibitor. Results of joint neutron and x-ray refinement of crystal form II. *J Mol Biol* 180:301–329.
4. Eigenbrot C, Randal M, Kossiakoff AA (1990) Structural effects induced by removal of a disulfide-bridge: The x-ray structure of the C30A/C51A mutant of basic pancreatic trypsin inhibitor at 1.6 Å. *Protein Eng* 3:591–598.

Table S2. Conserved structural waters in wild-type, reference, and simplified BPTIs

Waters*	ASA, %	BPTI-20st	BPTI-[5,55]st	5PTI	Ligands distances, Å
5016	0	Y	Y	Y	Trp10-N (2.95 ± 0.04) Asn43-N (2.74 ± 0.8) Lys41-O (4.25 ± 0.2)
5017	0	Y	Y	Y	Trp10-O (2.8 ± 0.04) Lys41-N (2.92 ± 0.06) 3004-O (2.71 ± 0.07)
5019	0	Y	Y	Y	Pro8-O (2.81 ± 0.07) 3004-O (2.66 ± 0.08) Asn43-N (3.96 ± 0.3)
5023	0	Y	Y	Y	Ala11-O (2.78 ± 0.03) Val/Cys38-O (2.73 ± 0.05)
5043	1.2	Y	Y	Y	Cys5-O (2.87 ± 0.2) Leu6-O (3.54 ± 0.2) Tyr23-OH (2.88 ± 0.09)
5089	24	Y	Y	Y	Ile19-N (2.89 ± 0.05) Arg17-O (3.96 ± 0.16)
5121	12	Y	Y	Y	Gly14-O (2.76 ± 0.1) Gly12-O (2.68 ± 0.2) Gly36-N (3.76 ± 0.8)
5133	20.9	Y	Y	Y	Asp50-OD2 (2.7 ± 0.1) Ala/Lys46-N (2.83 ± 0.08)
5199	43	Y	Y	Y	Ala/Thr54-O (2.75 ± 0.3) Ala/Arg53-O (3.87 ± 0.3)
5271 [†]	9.7	Y	N	N	Tyr21-OH (2.69) Ile19-O (4.81)
5178 [†]	2.7	Y	N	N	Asn24-OD1 (3.21) Asn-24N (3.20) Ala26-N (2.96)

*Identities and ASA of water molecules are as in BPTI-20st structure.

[†]Waters observed only in BPTI-20st.

Table S3. Intra-atomic distances (Å) in the wild-type, reference, and simplified BPTIs

Atom pair	4PTI	BPTI-[5,55]st	BPTI-20st
C ^α _C/G14-C ^α _C/A38	5.69	5.28	4.93
C ^α _C/A30-C ^α _C/A51	6.40	5.97	5.95
C ^α _C5-C ^α _C55	5.73	5.43	5.72
OH.Y21-CG2.T/A32	3.79	3.86	
OH.Y21-CB.T/A32	5.21	5.38	4.62
CZ.F4-CG2.T/A54	3.75	3.80	
CZ.F4-CB.T/A54	5.24	5.23	4.35
CZ.F45-CB.T/A54	3.97	3.57	3.74